Global Momentum Confinement Times in Alcator C-Mod H- and I-Regime Plasmas

by

Michelle Victora

Submitted to the Department of Physics
in partial fulfillment of the requirements for the degree of

Bachelor of Science in Physics

at the

MASSACHUSETTS INSTITUTE OF TECHNOLOGY

June 2014

Signature redacted

Author .....
Department of Physics
May 9, 2014

Signature redacted

Certified by .....
Bruno Coppi
Professor
Thesis Supervisor

Signature redacted

Certified by .....
John Rice
Senior Research Scientist
Thesis Supervisor

Signature redacted

Accepted by .....
Nergis Mavalvala
Senior Thesis Coordinator, Department of Physics

Global Momentum Confinement Times in Alcator C-Mod H- and I-Regime Plasmas

by

Michelle Victora

Submitted to the Department of Physics
on May 9, 2014, in partial fulfillment of the
requirements for the degree of
Bachelor of Science in Physics

Abstract

Using a spatially-resolving x-ray spectrometer system, the toroidal rotation velocity in Alcator C-Mod plasmas is measured and analyzed. At the L-H and L-I transition, there is a co-current movement in the toroidal rotation velocity.The propagation of this rotational velocity from the edge to the core of the torus was measured following the L- to H- and L- to I-mode transitions. A hyperbolic tangent fit was used to determine a single variable for rise time in rotational velocity. The hyperbolic tangent fit parameter acts as a proxy for the global momentum confinement time, which is then compared to other plasma parameters. Through this comparison, we found an decrease in rise time in correlation with increasing density(n)/current(I), particularly distinctive in the range of 1-2.5 $\cdot 10^{20}$ (MA$\cdot$ m^3)$^{-1}$. Due to a lack of overlap in density between I- and H-mode, we find this may be indicative of an overall decrease in rise time between L- to I- and L- to H-mode transitions. In order to explore this possibility, we must achieve I-mode runs with the same current and density as H-mode to determine if there is still a decrease between the two transitions.

Thesis Supervisor: Bruno Coppi
Title: Professor

Thesis Supervisor: John Rice
Title: Senior Research Scientist

Acknowledgments

I would like to thank John Rice for all his help in guiding my work as a UROP, and supervising this thesis. He has been both a friend and mentor in this process, and he has been patient with me through the entirety of my physics career underneath his counsel. I owe him a great deal for the advancement of my knowledge and enthusiasm for plasma physics. He has also provided an incredible amount of support through the course of my thesis work. I would also like to thank Professor Bruno Coppi for his work as my thesis advisor. Without him, I would never have been part of this incredible project. He was a source of strength, and a guidance for my theoretical understanding of the spontaneous rotation phenomenon underlying my research. Beyond that, I need to recognize all the scientists and engineers at the PSFC for the resources they have provided ranging from raw data to skeleton code to general guidance and support, including John Walk for the sharing of his thesis work, and Ted Golfinopoulos, for answering questions and providing extremely useful Matlab code. Finally, I would like to thank my friends and family for all they've done for me throughout the course of my MIT career.

Contents

List of Figures

List of Tables

Chapter 1

Introduction

At a time when consumer demands are rapidly increasing for a very much expanding population, it is important to continue exploring and discovering new and better ways of producing energy. Energy can be seen as directly proportional to quality of life as it is necessary for food, heat, lighting, transportation, etc. Right now, our main generation of energy is from burning fossil fuels, non-renewable resources that cannot be sustained forever.

Currently, our main electricity-generating resource is coal, which offers high availability and low-cost production. However, there are many drawbacks of using coal as a resource, the main disadvantage being environmental. Since coal is a fossil fuel, using any of it to burn for electricity leads to the unavoidable generation for CO_2, which is largely responsible for the greenhouse effect. Continuous CO_2 buildup over time will lead, and already has led, us to global warming, and cannot be sustained if we are to keep our planet healthy.

Oil is another fossil fuel, which has great portability and large energy content. However, oil does have limitations – like, coal, oil also produces greenhouse gases, lending to an increase in global warming. In addition, we procure the majority of our oil from politically unstable regions. Unnecessary warfare and military intervention has been driven by motivations not wholly unrelated to oil and its consumers. Beyond that, though, there is the undeniable future of our community hitting peak oil, when the maximum rate of petroleum extraction is reached. After this point, the rate of

production is expected to enter a stage of terminal decline. There is some consensus that we have already reached peak oil, and have entered this stage. If this is indeed the case, then necessity begs us to produce a longer-lasting, and ultimately cleaner source of energy for our future.

Traditional fission nuclear power plants are attractive sources of energy due to their low emissions and high efficiency, but they suffer from difficulties in fissible fuel accquisition and radioactive waste storage. Beyond that, their existence also promotes the spread of weapons-applicable nuclear technology and information to nations not recognized as "Nuclear Weapon States" by the *Treaty on the Nonproliferation of Nuclear Weapons*. No matter the benefits of fission nuclear power plants, we must admit the negative environmental and social consequences of their use.

Because of such non-maintainable energy sources, we look to fusion energy as a means to produce power. Fusion energy is safe, both for people and the environment, and also has a large amount of reserves. Because of these advantages, understanding what goes into creating this energy is a very noble and important cause. The key issue in achieving fusion is how to confine the plasma. Due to the high temperature required to overcome coulomb repulsion, plasma cannot be in direct contact with solid material, so it has to be located in a vacuum – however high temperatures also cause the plasma to expand, meaning we must find a way to act against this pressure. We have observed three different types of confinement: gravitational, inertial, and magnetic. Inertial and magnetic confinement have both been explored as methods of generating fusion power.

1.1 Alcator C-Mod

The Alcator C-Mod tokamak uses magnets to confine the plasma in a torus (see Fig. 1-1). Poloidal field magnets control the plasma's shape and position while toroidal field magnets combine with the poloidal field to produce a stable container for the plasma. The Alcator C-Mod has major radius $R = .68m$, minor radius $a = .22$ m, toroidal field $B_T \leq 8.1$ T, plasma current $I_P \leq 2.01$ MA [1]. The rest of the plasma

parameters are listed in Appendix A. A number of tools on the machine is available for further examination of plasma parameters. These include Thomson scattering diagnostics to probe plasma temperature and density, inteferometer arrays measuring radial-resolution plasma density, and an array of X-ray spectrometers, more intimately explained in the next section. Typical discharges last on the order of 2 seconds.

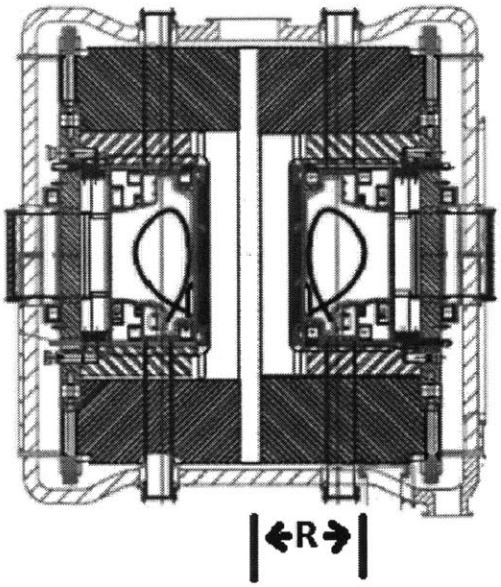

Figure 1-1: Cross-section view of C-Mod, from [3]. The red lines show the last closed magnetic flux service within the vacuum chamber. The blue lines indicate the plasma boundary.

1.2 X-Ray Spectroscopy

The X-ray spectrometers are capable of measuring ion and electron temperature, impurity density, and rotational-velocity data. In order to determine the rotational velocity of the plasma, an X-ray spectrometer was first used to observe the spectrum of various elements. The spectrometer uses a spherically bent crystal imaging arrangement that, in summary, allows for a pair of perpendicular line foci instead of a single focal point[2]. This allows for simultaneous measurement of spectra from multiple lines of sight through a plasma, which makes spectral tomography inversion feasible.

The spectrometer measures radiation from highly ionized charge states of argon, dominant states being H-like, He-like, and Li-like. By running locked mode discharges, we can obtain nonrotating tearing modes that act as a brake on toroidal rotation. If the plasma is not rotating, the emission lines are not Doppler shifted – these lines can be used to obtain a spectral calibration using published wavelengths of known emission lines. Once this calibration is obtained, we can measure the Doppler shift to calculate the impurity flow velocity and therefore obtain a reading of the rotational velocity of the plasma. We have verified stationary plasmas using independently calibrated spectrometers. The Doppler shift is given by

$$\lambda = \sqrt{\frac{1+\beta}{1-\beta}}\lambda_0 \tag{1.1}$$

where $\beta = v/c$, v is the source velocity, and λ_0 is the rest wavelength. Figure 1-2 shows the layout of the final spectrometer design. This layout includes four detectors that give us views of both the top and bottom of the plasma cross section, allowing us to distinguish between line shifts caused by poloidal and toroidal rotation.

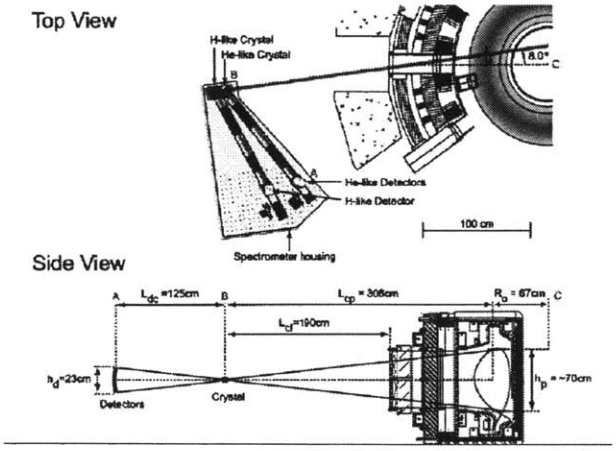

Figure 1-2: A top and side view of the HIREX array (x-ray spectrometer set-up). [4]

1.3 Argon Emission

Argon is the most commonly chosen impurity for observation because it radiates in an appropriate range of the x-ray spectrum for the temperature range of interest. The

density of H- and H-like states is dependent on temperature, among other things, which, in turn, depends on the radius in the plasma. The spectra are relatively bright and simple, and the impurity concentration can be carefully monitored and administered by gas puffing, so the level of argon can be easily controlled. Beyond that, argon is an inert gas, so we can use it to avoid unwanted chemical reactions that might interfere with experiments. The spectral lines are listed in Table 1.1. The charge state is determined by the balance between ionization and recombination (radiative and dielectronic), see Fig. 1-3. Graphs of both the dielectric and radiative recombination rate as functions of temperature for various charge states of argon are included in Appendix B.

Line Name	Charge State	Transition	Wavelength (Å)
ω	He-like Argon (Ar^{16+})	$1s2p\,^1P_1 \rightarrow 1s^2\,^1S_0$	3.9492
4C	Ne-like Molybdenum (Mo^{32+})	$4d \rightarrow 2p$	3.739
Ly α_1	H-like Argon (Ar^{17+})	$2p \rightarrow 1s$	3.731

Table 1.1: Spectra emission lines of interest, and their respective transitions and wavelengths

The temperature range is such that Ar^{17+} is generally the most abundant in the core of the plasma, and Ar^{16+} is the most abundant further out in the plasma. The ionization energy describes the amount of energy required to remove an electron from the atom or molecule in its gaseous state.

The charge state is determined by the balance between ionization and recombination (radiative and dielectronic). Graphs of the dielectric, recombination, and ionization rate as functions of temperature for various charge states of Ar are included in Appendix B.

As can be discerned from Fig. 1-3, above 500 eV, all Ar ions are stripped to about Ar^{14+} or higher. This, combined with the simplicity of argon's x-ray spectra, is another reason for using Ar^{17+} and Ar^{16+} for our measurements.

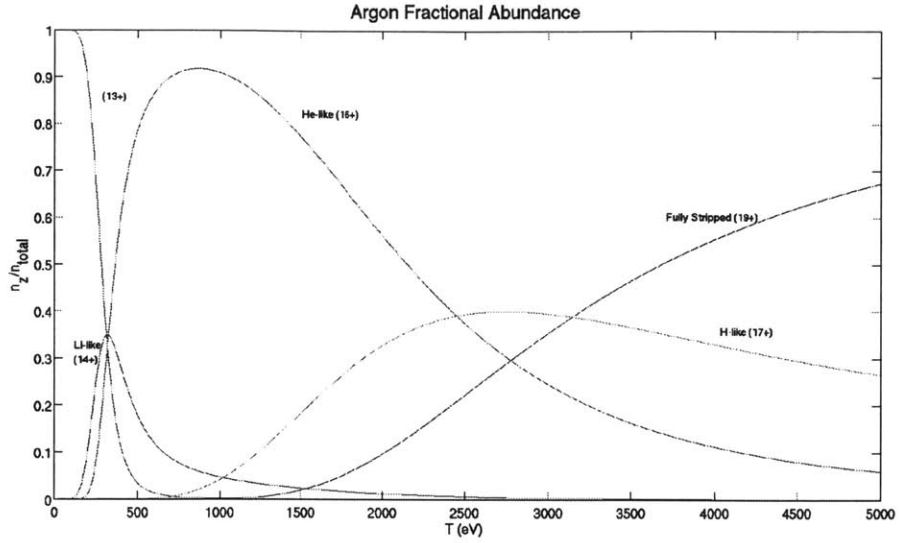

Figure 1-3: Fractional abundance against temperature for various charge states of Ar. [5]

1.4 Rotation and Rotation Profile Shape

We are interested in rotation and the rotation profile shape for a few reasons. First of all, a gradient of plasma rotation can help suppress turbulence, which, in turn, helps improve confinement (turbulence degrades confinement). Confinement refers to both particle and energy losses and the reduction of those losses through various means such as transport barriers.

We are also interested in the absolute magnitude of velocity. Rotation helps suppress MHD modes (resistive wall modes) which lead to disruptions. In these resistive wall modes, the resistivity of the plasma can deteriorate the plasma confinement [6].

1.5 Plasma Confinement Modes

In general, plasmas during discharges on the Alcator C-Mod tokamak are held in three general confinement modes. In low-energy confinement (L-mode), the particle and energy confinement times deteriorate over the course of the discharge. In contrast, the high-energy confinement (H-Mode), which exhibits greatly improved particle and energy confinement. I-Mode (in turn) exhibits a greatly improved energy confinement

with a relatively low particle confinement, thus achieving plasmas capable of fusion without high impurity retainment. Both the mechanism by which H-mode forms, and by which I-mode forms, are complex and not fully understood.

During H-mode and I-modes, a sharp increase in toroidal and poloidal rotation in the plasma has been observed in a variety of axisymmetric plasmas, discovered first over two decades ago by Hallock *et al.* on the ISX-B device. The observed velocities, or "spontaneous rotation" phenomenon, were confirmed to have magnitudes, directions, and radial distrubutions that are consistent with the excitation of modes that have a key role in the confinement properties of the considered plasmas. Professor Bruno Coppi theorized that the phenomenon is connected to the excitation of collective modes associated with these properties. Angular momentum is extracted from the plasma column from which these radially localized modes grow. The background plasma, in turn, must recoil in the direction opposite to that of the mode phase velocity, and this recoil angular momentum is then redistributed inside the plasma column mainly by the combination of an effective viscous diffusion and an inward angular momentum transport velocity. The rotational momentum increase is seen to propagate from the edge of the plasma column inwards to the core.

Chapter 2

Plasma Dynamics and Transport

In this section, I discuss the mechanics of plasma rotation and the momentum transport that is responsible for this behavior. In the Methodology section, we explore the mechanics of this momentum transport with respect to various parameters governing a plasma "shot". In particular, we study the "rise time", or time it takes for the plasma velocity to switch from its initial steady-state velocity to settle at its final steady-state velocity. We also look at the it takes for the density of the plasma to rise to a new steady density, as well. Here, though, we simply discuss the theory behind this motion.

2.1 Rotation and Rotation Profile Shape

We are interested in rotation and the rotation profile shape for a few reasons. First of all, a gradient of plasma rotation can help suppress turbulence, which, in turn, helps improve confinement (turbulence degrades confinement). Confinement refers to both particle and energy losses and the reduction of those losses through various means such as transport barriers.

We are also interested in the absolute magnitude of velocity. Rotation helps suppress MHD modes (resistive wall modes) which lead to disruptions. In these resistive wall modes, the resistivity of the plasma can deteriorate the plasma confinement [6].

2.2 Momentum Transport

In order to examine fully the rotation and the rotation profile shape, we have to understand what velocity looks like in a tokamak, and, more specifically, what velocity looks like in Alcator C-Mod. For example, in C-Mod we have no external momentum source. High confinement modes, or H-modes, are achieved either through Ohmic methods or by Ion Cyclotron Resonance Heating (ICRH). In general, momentum transport is modeled using three possible momentum transport coefficients – momentum diffusion, momentum pinch (convective flux), and additional terms associated with the excited modes of the plasma, including ion temperature gradient modes and other various curvature gradients. These latter two terms are regarded as non-diffusive, and they are independent of the velocity gradient.

Momentum transport may be modeled by

$$P_\phi \propto -D_{\mu\perp} \bigtriangledown v_\phi + V_{pinch} v_\phi + \triangle P_\phi^{modes} \tag{2.1}$$

where P_ϕ is the radial flux of toroidal momentum, and v_ϕ is the rotation velocity[7]. The first term serves as the diffusive term, while the second and third are regarded as non-diffusive, with V_{pinch} defined as the momentum pinch, and $\triangle P_\phi^{modes}$ in the form of a tensor, whose components are associated with modes excited in the considered plasmas.

2.2.1 Diffusion Term

Turbulence can have an important effect on the diffusive term, considering that this has a collisional component D_{NC}. Here, D_{NC} is a neo-classical term, proportional to $\rho_i^2 v_i$, where ρ_i is the transverse orbit radius of circulating particles, and v_i is the collision frequency. However, since there are non-diffusive terms in momentum transport, evaluation of the viscosity coefficient proves difficult. We evaluate the viscosity as "effective" viscosity by ignoring non-diffusive terms, essentially utilizing Fick's Law to calculate the viscosity coefficient. Naturally, it is most convenient to effectively make source free measurements. We achieve this through Ohmic methods

or by Ion Cyclotron Resonance Heating. Through heating up the plasma in this fashion, we achieve a transition from L-mode to H-mode or I-mode. If the rotation profile is flat, then diffusion is the only active momentum transport coefficient.

2.2.2 Momentum Pinch

The 2000 IAEA paper by B. Coppi [8] was the first to explain spontaneous rotation by the effects of excited collectiive modes extracting angular momentum from the background plasma. The included Momentum Pinch is a non-diffusive process, whose magnitude depends on the velocity of the plasma. It is used to describe the peaking of toroidal rotation that can sometimes occur, which could not be explained simply by momentum diffusion. The momentum pinch was first experimentally determined in 1994 by K. Nagashima *et al.* using neutral beam injections on the JT-60U tokamak [9]. At the same time, the momentum pinch was independently introduced in the context of angular momentum transport in astrophysics by B. Coppi[10]. In fact, both papers argued that the angular momentum pinch had to be the particle pinch term that had been introduced in 1978 [11] in order to reproduce the observed particle density profiles. We can think of the momentum pinch as similar to the convection process we are familiar with seeing in heat transfer through liquids.

2.2.3 Additional Mode-Driven Terms

There are some interesting phenomena in rotation velocity (such as spontaneous rotation reversal) that cannot be explained solely by the momentum pinch. Here, the final term, ΔP_{ϕ}^{modes} comes in to play, which is a non-diffusive momentum term that is sensitive to the various modes excited within a driven plasma which enhance particle and thermal energy transport across the magnetic field. It has been confirmed experimentally [12],[13], that observed velocities in the plasma have magnitudes, directions, and radial distributions that are consistent with the excitation of modes which have a key role in the confinement properties of the considered plasmas. Such modes can sometimes be seen as driving instabilities within a plasma, such as that driven by a ra-

dial gradient of the electron temperature or by the electron drift in the "unfavorable" curvature of magnetic field lines [14]. Other modes of energy transport come in the form of impurity driven modes, driven by impurity density gradients along the radius of the magnetically confined plasma [15].The dominating modes in an inhomogeneous confined plasma are represented by the radial temperature and density gradients of the hot ion population, as well on the electron temperature gradient [16].

2.3 Confinement Modes

The plasma exists in one of three general confinement modes. In low-energy confinement (L-mode), particle and energy confinement times are low over the course of the discharge. H-mode refers to a mode of plasma operation with high energy confinement and high particle confinement, which results in a sudden increase in plasma density and plasma pressure. I-mode [17], on the other hand, is a mode achieved with the high energy confinement of H-mode and the low particle confinement of L-mode. I-mode is desirable because it features an edge energy transport barrier without an accompanying particle barrier – this results in reduced impurity radiation. I-mode and H-mode plasmas have both displayed intrinsic rotation with similar edge origin and global pressure scaling. Both plasmas have similar edge ∇T, but completely different edge ∇n where T=temperature and n=density ([18]).

Figures 2-1 through 2-4 demonstrate general characteristics of various parameters in H-mode and I-mode plasmas. As we can see between Figures 2-1 and 2-2, the progression of density can distinguish between an H-mode and I-mode plasma, with the H-mode characterized by achievement of a short but steep rise in density after the initiation of ICRF power, followed by a density "plateau". I-mode density plateaus after the onset of ICRF power, with no increase. Figures 2-3 and 2-4, however, demonstrate that H-mode and I-mode achieve similar levels of stored energy.

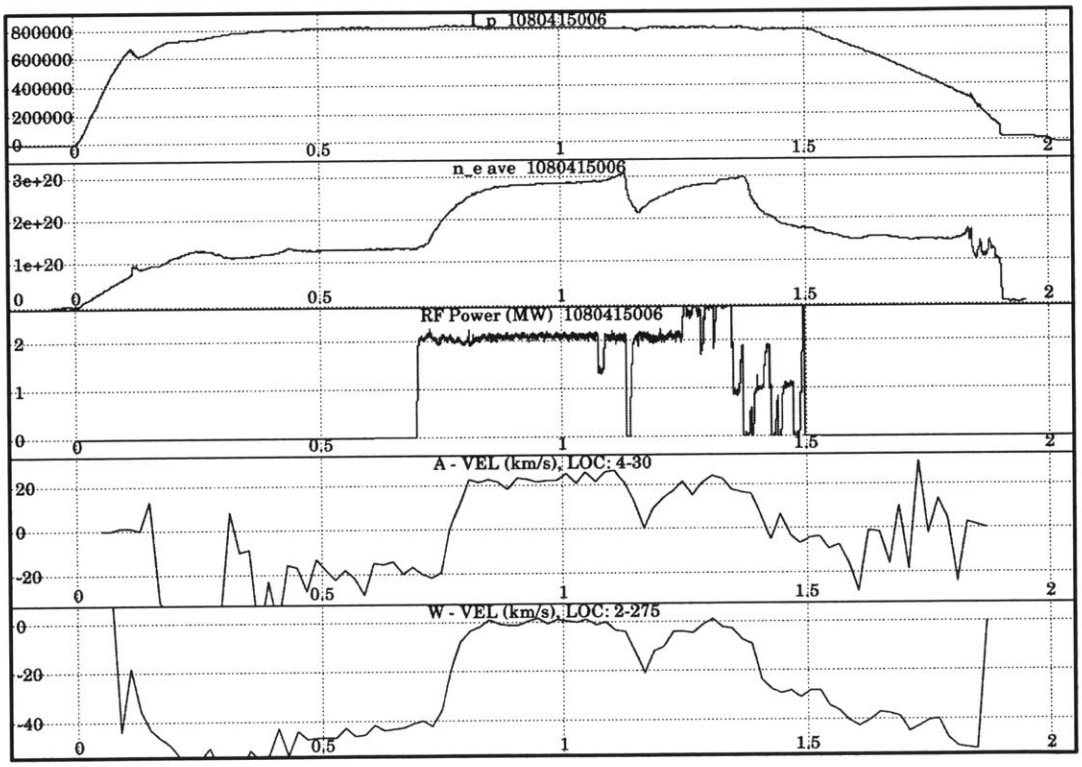

Figure 2-1: From top to bottom, a plot of current (MA), density (m^{-3}), rf power, (MW), H-like velocity (km/s), and He-like velocity (km/s). Plots taken from H-mode plasma.

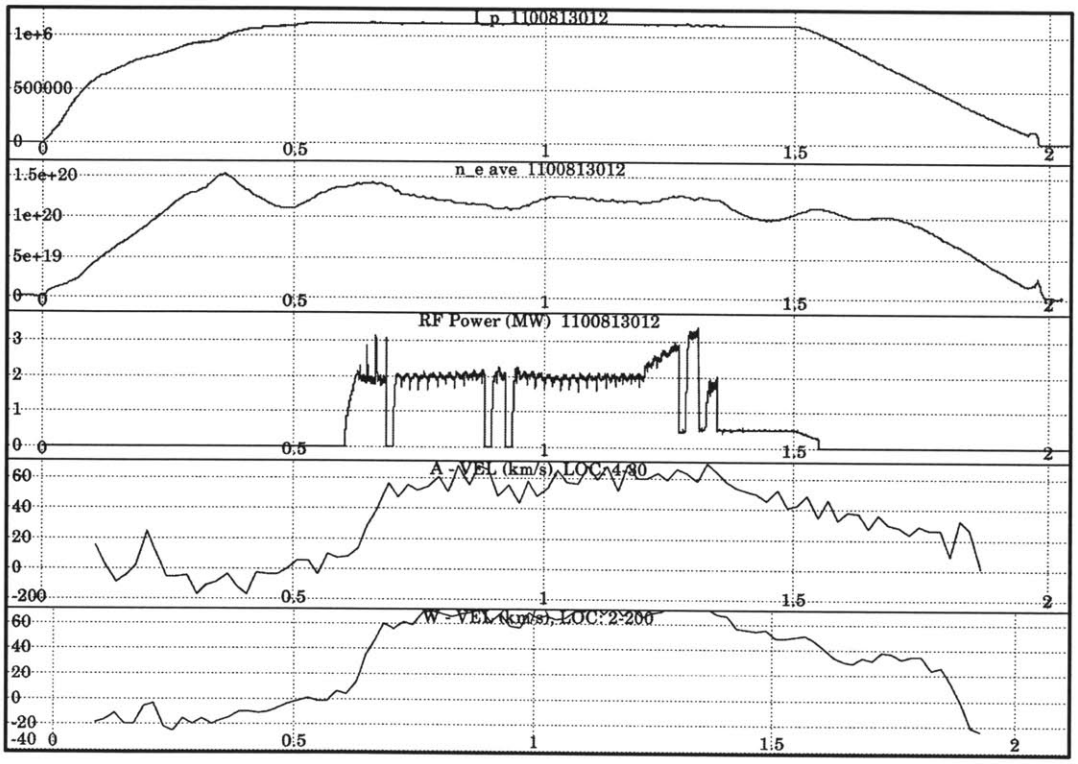

Figure 2-2: From top to bottom, a plot of current (MA), density (m^{-3}), rf power, (MW), H-like velocity (km/s), and He-like velocity (km/s). Plots taken from I-mode plasma.

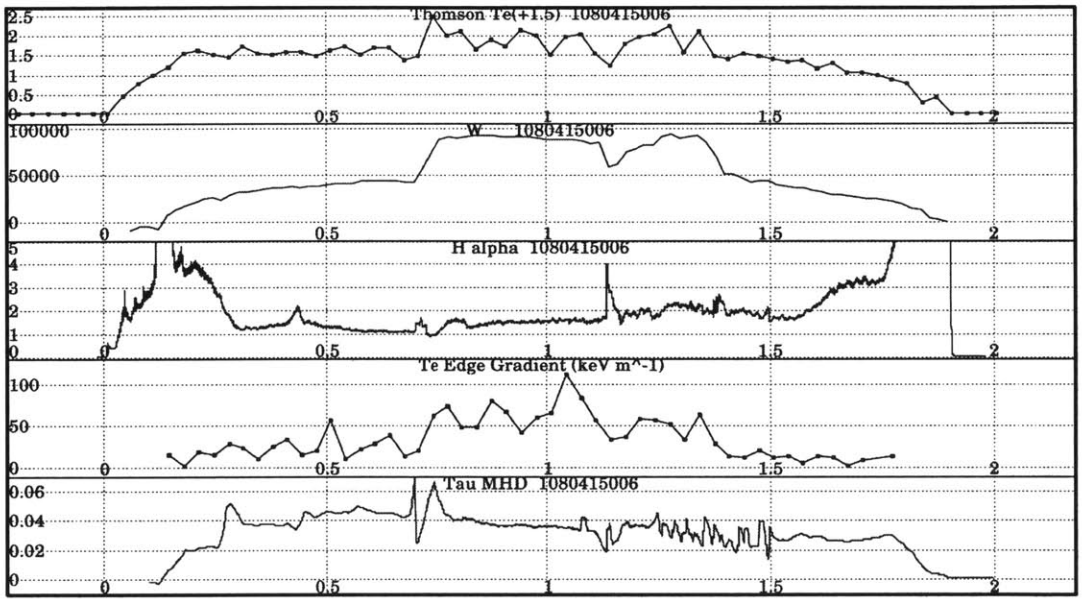

Figure 2-3: From top to bottom, a plot of plasma temperature, stored energy, (MW), H_α, temperature edge gradient, and experimental energy confinement time. Plots taken from an H-mode plasma

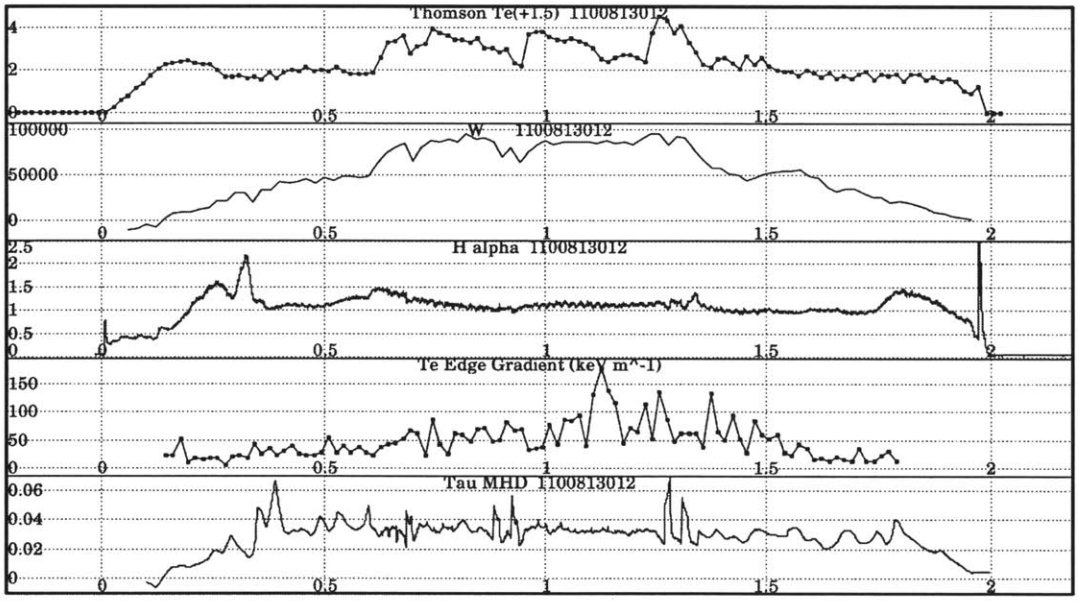

Figure 2-4: From top to bottom, a plot of plasma temperature, stored energy, (MW), H_α, temperature edge gradient, and experimental energy confinement time. Plots taken from an I-mode plasma

Chapter 3

Experimental Observations and Conclusions

3.1 Methodology

Our goal here is to study the transition from L-mode to H-mode (Fig. 2-1) or I-mode (2-2) and the rise in co-current plasma velocity correlating to this shift. The transition is very abrupt, beginning at the outer edge of the plasma, coinciding with the formation of a steep temperature and/or density gradient. A large temperature pedestal gradient is present in the I-mode and H-mode transition. However, in contrast with H-mode, there is no significant density gradient in I-mode compared to L-mode [17]. The transition between modes moves from the edge to the core, which we can observe in the difference of velocity rise onset between the edge and the core.

3.1.1 Computer Model

In this experiment, we looked at fits to the velocity time history made with hyperbolic tangents. Hyperbolic tangents were chosen so as to provide us a one-parameter fit allowing us to easily find correlations between various qualities of plasma runs. Hyperbolic tangents also provided a relatively accurate fit to the rise times we looked at. The equation used was

$$v = v_0 \frac{1 - e^{-t/\tau}}{1 + e^{-t/\tau}} \tag{3.1}$$

where v=magnitude of velocity, t= time in seconds, and τ was the fitted time constant to determine the rise time in velocity of the plasma. The fits were done by a Matlab program solving the hyperbolic tangent model using the data supplied from a particular shot. This method was chosen in order to produce a reasonable estimate of the time constant with minimal error. The velocity data being fit was truncated in order to focus the fit on the region of interest (i.e., the change from one steady-state velocity to the next). User-defined values suggested a starting and ending velocity, and the program produced a hyperbolic tangent fit that minimized the error χ^2 where

$$\chi^2 = \sum_{i=1}^{k} \frac{(O_i - E_i)^2}{E_i} \tag{3.2}$$

Here, O_i represents the observed point, and E_i represents the expected value from the model. Example fits are produced below in Figures 3-1 and 3-2. Both shown fits, were taken from W-VEL (He-like argon), but M-VEL(Ne-like molybdenum) and A-VEL(H-like argon) were also analyzed.

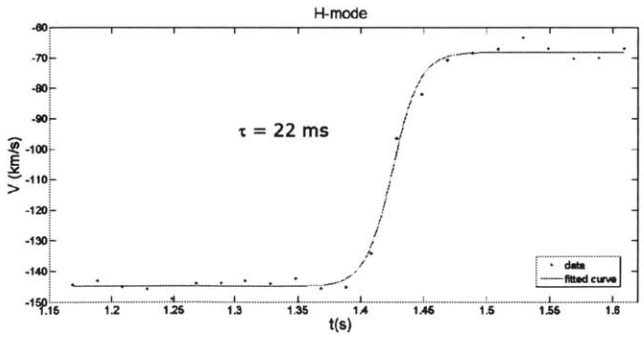

Figure 3-1: This is an example of a hyperbolic tangent fit. Transition was L-mode to H-mode, taken from W-VEL. τ = .0217 sec.

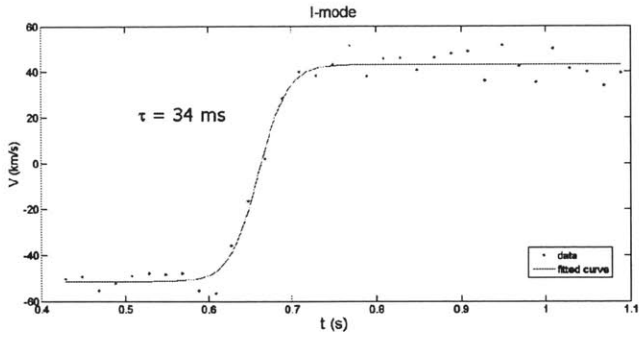

Figure 3-2: This is an example of a hyperbolic tangent fit. Transition was L-mode to I-mode, taken from W-VEL. $\tau = .0459$ sec.

3.2 Observations

Once fits were performed on a large number of shots, time constants τ were compared against parameters of density(n)/current(I). This operational space was used in order to account for the covariance between density and current (see fig 3-3). Points represent data for I-Mode and H-Mode; the lines represent an average time constant for a particular range. Here, we can see an obvious positive correlation between current and density in H-mode and a potential positive correlation in I-mode. Fig. 3-5 plots our calculated time constants against n/I, taken from a variety of shots. We see in the range of 1-2.5 $\cdot 10^{20}$ (MA $\cdot$ m^3), that the average time constant increases with respect to n/I, coinciding with a change from I-mode dominated runs to H-mode dominated runs. By using a reduced set of points with I limited to a range of 6-9 Amperes, we were able to produced Fig. 3-4, a depiction of τ against density. Here, we see that, in fact, τ is relatively independent of n. This is particularly clear for H-mode; I-mode suffered from wide scatter in its τ values, and so may not be entirely conclusive.

Further exploration included fitting hyperbolic tangents to the density rise time itself, and noting correlations between density rise time and current, density, or velocity rise times. As can be seen in Fig. 2-1, once the RF power has been turned on, the density follows a hump-like rise in H-mode, not seen in I-mode. Using the same method used to determine the velocity rise time in H-mode and I-mode, fits were made to find a time constant proportional to the slope of the density rise time

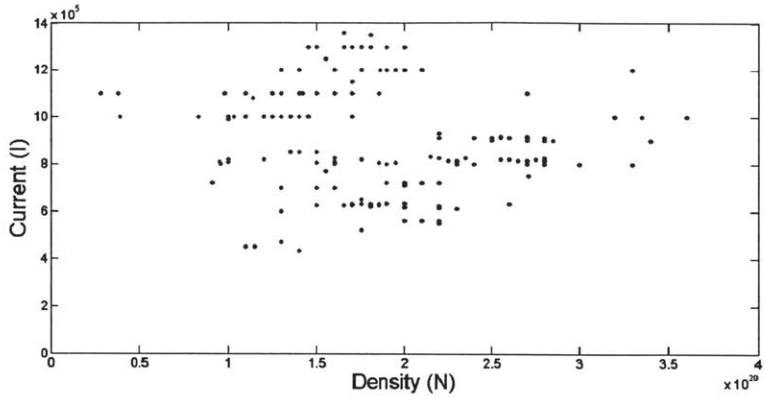

Figure 3-3: Current against density plotted over a variety of H-mode and I-mode plasma runs, I-mode in red, H-mode in blue.

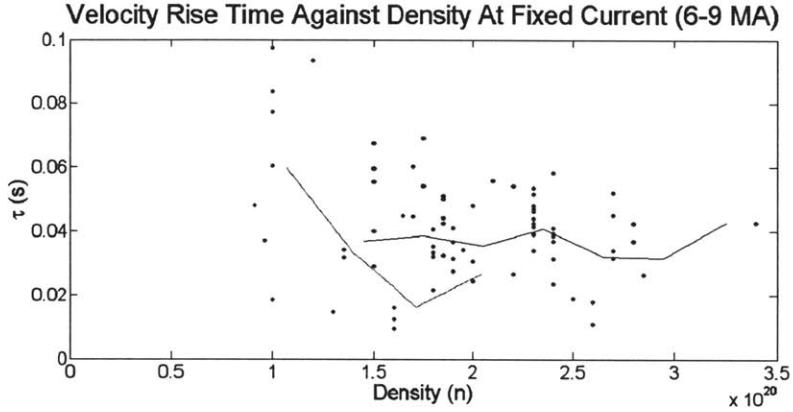

Figure 3-4: Velocity rise time plotted against density from a variety of H-mode and I-mode plasma runs, I-mode in red, H-mode in blue. Current has been limited to range from 6-9 MA.

in H-mode. Figures are shown below, plotting current, density, and velocity rise time against density rise time.

Linear fits to the plots have been created using a linear regression scheme in Matlab. In order to comply with the physical model, the line was constrained to cross at the origin. As we can see, there is a slight positive correlation ($3928 \cdot 10^{-8}$ s/I) between current and density rise time, and a much more defined, albeit slighter ($1.359 \cdot 10^{-22}$ s $\cdot M^3$) positive correlation between average density and density rise time in H-mode. Such correlations could be a result of the higher density and current corresponding to a higher ionization rate in plasma particles. In particular, as the speed of the particles increases (i.e., current increases), the likelihood of collision also

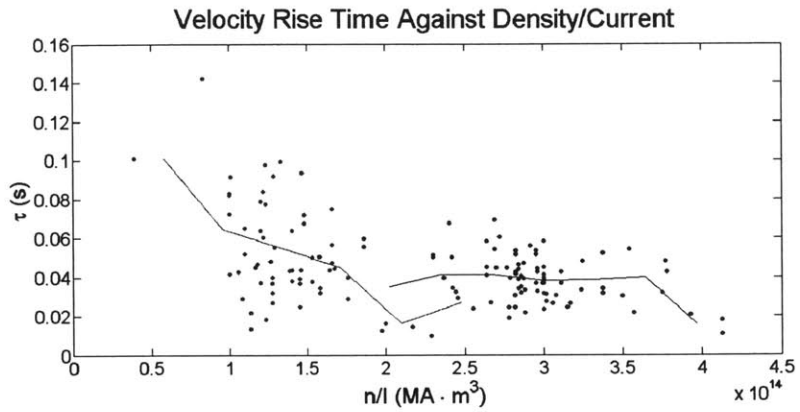

Figure 3-5: Time constant plotted against density/current. Points taken from a variety of shots from W-VEL, M-VEL, and A-VEL. I-mode in red, H-mode in blue.

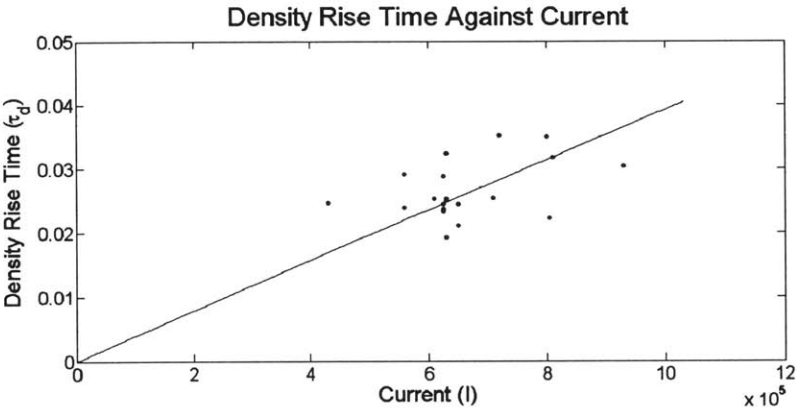

Figure 3-6: Density rise time plotted against current in H-mode.

grows and the overall plasma heats up more quickly. In turn, this may contribute to a higher achieved density by the time the plasma has reached its new steady-state in H-mode. Due to the correlation between current and density, it is difficult to separate the two dependences. However, while the density to current line calculated in Fig. ?? has a slope of $9.5879 \cdot 10^{19}$ n/I, the relation between the two correlations in density rise time is only $2.890 \cdot 10^{14}$ n/I. This suggests that the density rise time is dependent on both current and density in separate functions. Velocity rise time does not exhibit an obvious positive or negative correlation with density rise time.

An important note to make is that the hyperbolic tangent is, in theory, not the best model for change in velocity. In fact, Bessel functions, given by

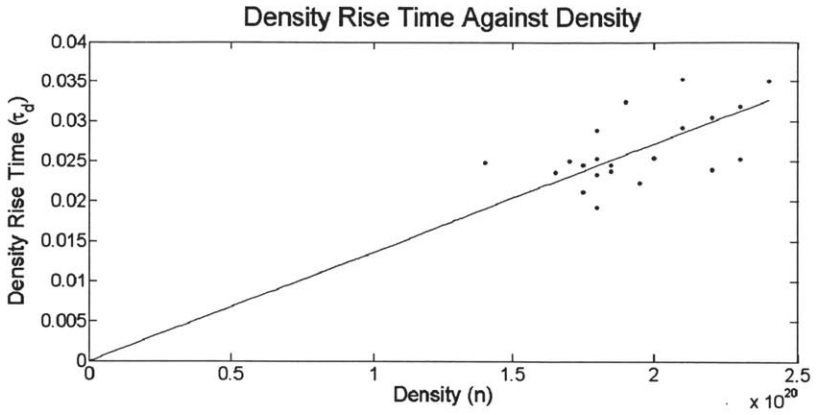

Figure 3-7: Average density rise time plotted against density in H-mode.

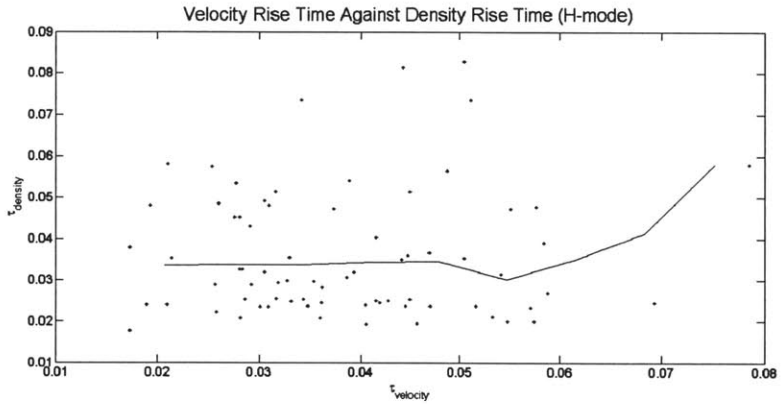

Figure 3-8: Velocity rise time plotted against density rise time in H-mode.

$$J_\alpha(x) = \sum_{m=0}^{\infty} \frac{(-1)^m}{m!\Gamma(m+\alpha+1)} \left(\frac{x}{2}\right)^{2m+\alpha} \tag{3.3}$$

behave more correctly, by solving a simplification of the momentum diffusion equation, given by the model

$$\frac{\partial}{\partial t} - D_\phi \left(\frac{\partial^2}{\partial r^2} v_\phi + \frac{1}{r} \frac{\partial}{\partial r} v_\phi \right) = 0 \tag{3.4}$$

By theoretical arguments, a Bessel function has a strong argument for being the best fitting function to this particular set of data. The choice of a hyperbolic tangent fit, in this particular study, was a simplification made to characterize a single variable time parameter over a large amount of shots. The main goal of the study was to compare the time it took for rotation velocity change from one steady-state to another,

and this comparison was easily and elegantly achieved by using a hyperbolic tangent to fit and analyze the data. Now that certain correlations have been realized in this analysis, the next step could include gaining a more accurate estimate of each rise time value, using a series of Bessel functions to produce a recursion fit for the velocity profiles.

3.3 Conclusion

In I-mode and H-mode discharges on the Alcator C-mod tokamak, toroidal rotation and density changes were measured using Thompson Scattering and HiReX SR, a spatially resolving X-ray spectrometer. Velocity rise times were measured using a simple hyperbolic tangent model for the toroidal rotation profile.

3.3.1 Results

We see an implied independence of velocity rise time (τ) from n (Fig. 3-4) and n/I (Fig. 3-5). There is a possible positive correlation between τ and n, present in the velocity rise time in Fig.3-4, ranging from 1.5 to 2.25 $\cdot 10^{20}$ m $^{-3}$. In Fig. 3-5, we see an increase of time constant between H-mode and I-mode in the region where they overlap in n/I. We also see a strong positive trend between current vs. density, density rise time vs. density, and density rise time vs. current.

3.3.2 Future Work

Future possibilities for exploration include a way to fuel I-mode so that we can achieve I-mode runs with the same density as H-mode. This method involves gas puffing to adjust the density while maintaining that current level. Once we achieve this, we can then revisit this analysis and explore the correlation between rise time and n/I independent (or perhaps with respect to) H-mode and I-mode.

Appendix A

Alcator C-Mod Parameters

Parameter	Value/Range
major radius	.68 m
minor radius	.22 m
plasma volume	1 m^3
plasma surface area	7 m^2
toroidal field	$\leq$ 8T
plasma current	$\leq$ 2MA
elongation	$\leq$ 1.9
ICRF power	8 MW, 50-80 MHz
LHRF power	2 MW, 14.6 GHz
normalized pressure	$\leq$ 1.8
absolute plasma pressuree	$\leq$ 0.2 M Pa
density	$< 10^{21}/m^3$
temperature	<9 keV

Appendix B

Ionization and Recombination Rates

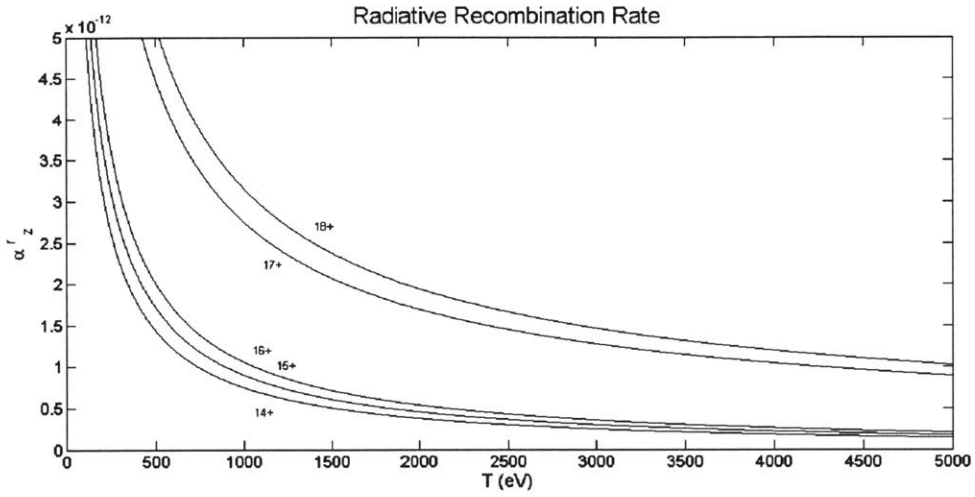

Figure B-1: The radiative recombination rate against temperature for various Argon charge states [5]

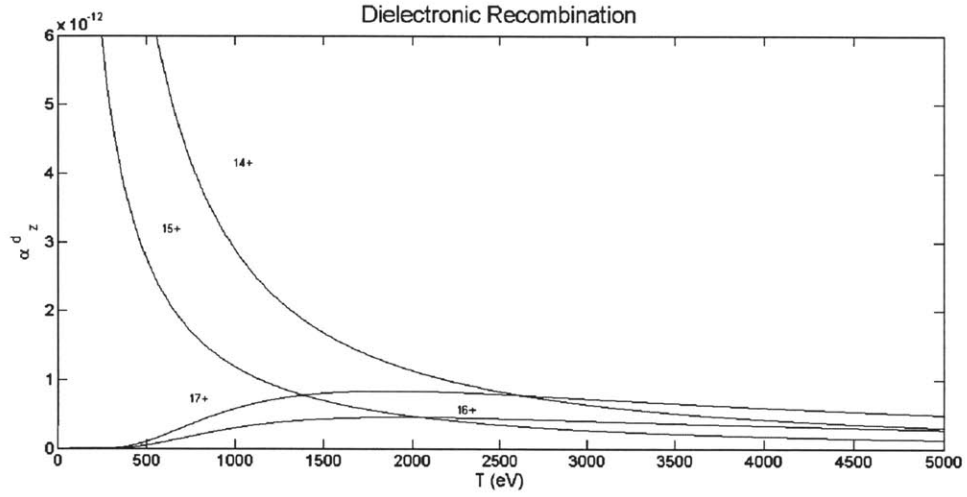

Figure B-2: The dielectronic recombination rate against temperature for various Argon charge states [5]

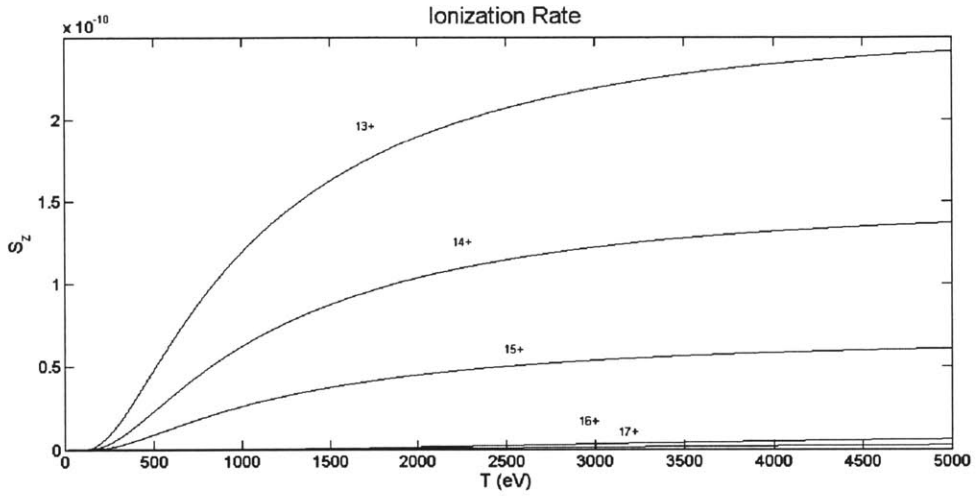

Figure B-3: The ionization rate against temperature for various Argon charge states [5]

Bibliography

[1] Marmar, E.S. "The Alcator C-Mod Program." *Fusion Science and Technology* 51.3 (2007): 261-265.

[2] Hill, K.W., M.L. Bitter, S.D Scott, A. Ince-Cushman, M. Reinke, J.E. Rice, P. Beiersdorfer, M.F. Gu, S.G. Lee, Ch. Broennimann, and E.F. Eikenberry. "A Spatially Revolving X-Ray Crystal Spectrometer for Measurement of Ion-Temperature and Rotation-Velocity Profiles on the Alcator C-Mod Tokamak." *Review of Scientific Instruments* 79, 10E320 (2008)

[3] Walk, John. *The L- to H-Mode Transition and Momentum Confinement in Alcator C-Mod Plasmas.* Thesis / Dissertation ETD, 2011. Print.

[4] Ince-Cushman, Alexander Charles. *Rotation Studies in Fusion Plasmas via Imaging X-ray Crystal Spectroscopy.* Thesis. Massachusetts Institute of Technology, Dept. of Nuclear Science and Engineering, 2008.

[5] Lee, W. Davis. *Experimental Investigation of Toroidal Rotation Profiles in the Alcator C-Mod Tokamak.* Thesis. Massachusetts Institute of Technology, Dept. of Nuclear Engineering, 2003. N.p.: n.p., n.d. Print.

[6] Martynov, Andrey. *Ideal MHD Stability of Tokamak Plasmas With Moderate and Low Aspect Ratio.* Thesis. Institute of Physical Engineering of Moscow, 2005.

[7] Ida, K., and J. E. Rice. "Rotation and Momentum Transport in Tokamaks and Helical Systems." *Nuclear Fusion* (2014).

[8] Coppi, B. "Accretion Theory of 'Spontaneous' Rotation in Toroidal Plasmas." *Nuclear Fusion* 42.1 (2002): 1-4.

[9] Nagashima, K., Y. Koide, and H. Shirai. "Experimental Determination of Non-diffusive Toroidal Momentum Flux in JT-60U." *Nuclear Fusion* 34.3 (1994): 449-54.

[10] Coppi, B. "Astrophysical and Laboratory Experiments and Theories on High Energy Plasmas." *Plasma Physics and Controlled Fusion* 36.12B (1994): B107-121.

[11] Coppi B. and Spight C. 1978 Phys. Rev. Lett. 21 1363

[12] B. P. Duval, A. Bortolon, L. Federspiel, F. Felici and I. Furno et al. *Momentum Transport in TCV Across Sawteeth Events.* 23rd IAEA Fusion Energy Conference, Daejon, Korea, 2010.

[13] J.E. Rice, J.W. Hughes, Ph. Diamond, Y. Kosuga, Y.A. Podpaly, M. L Reinke, et al. *Edge Temperature Gradient as Intrinsic Rotation Drive in Alcator C-Mod Tokamak".* Plasmas, Phys. Rev. Lett. 106, 215001. 2011.

[14] Coppi, Bruno, and Gregory Rewoldt. "New Trapped-Electron Instability." *Physical Review Letters* 33.22 (1974): 1329-332. Print.

[15] Coppi, Bruno, Gregory Rewoldt, and Theo Schep. "Plasma Decontamination and Energy Transport by Impurity Driven Modes." *Physics of Fluids* 19.8 (1976): 1144. Print.

[16] Coppi, Bruno, and Dilip K. Bhadra. "Collective Modes in an Inhomogeneous Beam Injected Plasma." *Physics of Fluids* 18.6 (1975): 692. Print.

[17] Whyte, D.G., A.E. Hubbard, J.W. Hughes, B. Lipschultz, J.E. Rice, E.S. Marmar, M. Greenwald, I.Cziegler, A. Dominguez, T. Golfinopoulos, N. Howard, L. Lin, R.M. Mcdermott, M. Porkolab, M.L. Reinke, J. Terry, N. Tsujii, S. Wolfe, S.

Wukitch, and Y. Lin. "I-mode: An H-mode Energy Confinement Regime with L-mode Particle Transport in Alcator C-Mod." *Nuclear Fusion* 50.10 (2010: 105005). Print.

[18] Rice J.E. *et al.*, 2011 *Phys. Rev. Lett.* **106** 215001

[19] Bevington, Philip R., and D. Keith. Robinson. *Data Reduction and Error Analysis for the Physical Sciences.* New York: McGraw-Hill, 1992. Print.